ELSEVIER

Journal of Organometallic Chemistry 488 (1995) 115–125

Journal of Organometallic Chemistry

Anchoring rhodium(I) on benzoylthiourea-functionalized silica xerogels. Production of recyclable hydroformylation catalysts and the crystal structure of the model compound [Rh(cod)(Hbztu)Cl] ☆

Daniele Cauzzi [a], Maurizio Lanfranchi [a], Giovanna Marzolini [a], Giovanni Predieri [a], Antonio Tiripicchio [a,*], Mirco Costa [b], Roberto Zanoni [c]

[a] *Dipartimento di Chimica Generale ed Inorganica, Chimica Analitica, Chimica Fisica, Università di Parma, "Centro di Studio per la Strutturistica Diffrattometrica" del CNR, Viale delle Scienze 78, I-43100 Parma, Italy*

[b] *Dipartimento di Chimica Organica e Industriale, Università di Parma, Viale delle Scienze 78, I-43100 Parma, Italy*

[c] *Dipartimento di Chimica, Università di Roma "La Sapienza", Piazzale A. Moro 5, I-00185 Roma, Italy*

Received 10 June 1994

Abstract

Two benzoylthiourea-functionalized silica xerogels, $4.5SiO_2 \cdot SiO_{3/2}(CH_2)_3NHC(S)NHC(O)Ph$ (XGbztu) and $SiO_{3/2}(CH_2)_3NHC(S)NHC(O)Ph$ (XGbztu*) have been prepared from $(EtO)_3Si(CH_2)_3NHC(S)NHC(O)Ph$ by the sol–gel process. They are able to bind rhodium(I) species giving the composite materials Rh/XGbztu and Rh/XGbztu*, which are very active insoluble and recoverable catalysts for the hydroformylation of styrene. The anchored species undergo major changes during the catalytic cycles, particularly in the Rh/XGbztu system, whose iso/normal selectivity ratio gradually increased in the first five runs. Furthermore, $CH_3(CH_2)_2NHC(S)NHC(O)Ph$ (HBztu) has been studied as a model of the surface binding function. The structure of [Rh(cod)(Hbztu)Cl] [1], which represents a suitable molecular model for the anchored complexes, has been determined by X-ray diffraction.

Keywords: Rhodium; Xerogel; Crystal structure; Hydroformylation; ESCA; Supported catalyst

1. Introduction

One important goal of modern metal catalyst design is to combine the easy recovery of solid catalysts with the high activity and selectivity of soluble complexes [1–3]. This can be achieved by attaching the soluble catalyst to an insoluble support through a tethered ligand, thereby obtaining a so-called hybrid (heterogenized homogeneous) catalytic system [4]. The solid support is normally chosen on the basis of certain parameters such as inertness to reagents and products, mobility of the tethered functions, porosity, mechanical and thermal stability.

Extensive studies have been carried out on organic polymers as supports which can be functionalized rather easily with the desired ligand group: the most popular approach involves macromolecular phosphine as supports [4,5], although nitrogen ligands (amines [6] and nitriles [7]) have also been employed to functionalize polymers. Very recently, a new system based on macromolecular rhodium isocyanide complexes as catalyst precursors has been described and used in the direct synthesis of alcohols from n-olefins and syngas [8]. However organic macromolecular systems do not completely fulfill the requirements on supports, as their structures are not rigid and depend greatly on the temperature and the reaction medium.

These disadvantages can be overcome by anchoring a suitable ligand group L to a porous rigid system such as silica gel by reaction of the surface Si–OH groups with functionalized alkoxysilanes of the type $(RO)_3Si—(CH_2)_n—L$ bearing a suitable spacer aliphatic chain. Alternatively, it is possible to prepare insoluble func-

☆ Dedicated to Professor Fausto Calderazzo: on the occasion of his 65th birthday and in recognition of his important contributions to organometallic chemistry.

* Corresponding author.

[1] cod = 1,5-cyclooctadiene; Hbztu = *N*-benzoyl-*N'*-propylthiourea.

SSDI 0022-328X(94)00009-3

tionalized xerogels directly by the sol–gel process [9] via a one-step synthesis which consists of the hydrolysis and co-condensation of $(RO)_4Si$ (fourfold cross-linking) with the substituted alkoxide. In this way it is possible to obtain organic/inorganic hybrid materials of the type $nSiO_2 \cdot SiO_{3/2}$—$(CH_2)_n$—L with controlled density of ligating functions (depending on the molar ratio of the two starting reagents), offering the possibility of studying the catalytic activity of a particular metal complex as a function of the abundance of the donor groups on the surface. Furthermore, particular organic spacers, including bridging groups, can be chosen in order to modify the porosity of the inorganic network [10]. Generally this synthetic procedure provides robust materials with a higher content of available ligand groups than their silica-immobilized counterparts produced by reaction of an alkoxysilane with the surface silanol groups [11].

Depending on the nature of the metal species and on the process conditions, both anchored metal complexes with catalytic activity [12] and supported small metal particles [13] can be prepared starting from hybrid sol–gel materials. The phosphine group [12a,b,e,14] tethered to silica is still the most common binding function, but nitrogen [12d,15], oxygen [12f] and sulfur [16] ligands have also been used as surface modifiers.

Seeking new ancillary ligands for catalytic processes, we have recently found that the new thiourea-functionalized xerogels XGtu and XGditu, derived from $(EtO)_3Si(CH_2)_3NHC(S)NHPh$ and $(EtO)_3Si(CH_2)_3N\{C(S)NHPh\}(CH_2)_2NHC(S)NHPh$, respectively, by sol–gel methods are capable of binding palladium(II) [17], copper(I) and (II) [18], rhodium(I) [19] and metal carbonyl species, including clusters [20] by a coordinate linkage. In the case of the system Pd/XGtu, treatment with dihydrogen affords colloidal metal particles, as shown by transmission electron microscopy, with selective hydrogenating activity [17].

Continuing these investigations, we have now synthesized the potentially bidentate benzoylthiourea $(EtO)_3Si(CH_2)_3NHC(S)NHC(O)Ph$ as a precursor of the new functionalized xerogels XGbztu when sol–gel processed with $Si(OR)_4$, and of XGbztu* when processed alone. A pictorial view of the tethered benzoylthiourea function is shown in Scheme 1. The non-siloxanized thiourea $CH_3(CH_2)_2NHC(S)NHC(O)Ph$ (Hbztu) has been used as a model for the surface-binding function. Its crystal structure [21a] exhibits an N—H · · · O intramolecular hydrogen bond like that shown in Scheme 1 for XGbztu.

This paper describes the anchoring reactions of $[\{Rh(cod)Cl\}_2]$ (cod = 1,5-cyclooctadiene) and of $[\{Rh(CO)_2Cl\}_2]$ with XGbztu and its superfunctionalized analogues XGbztu* to give rhodium(I) species tethered by an Rh—S coordinate linkage. These hybrid systems are promising precursors for active recyclable hydroformylation catalysts, styrene being converted quantitatively into the corresponding linear and ramified aldehydes. Furthermore, the structure of [Rh(cod)(Hbztu)Cl] (**1**), which represents a suitable molecular model for the anchored complexes, has been determined by X-ray diffraction.

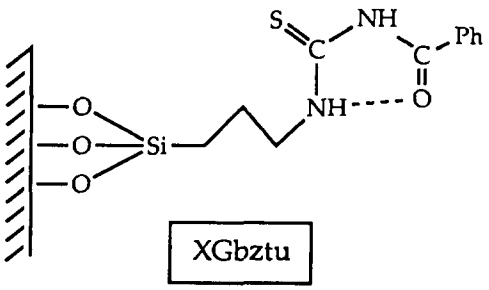

Scheme 1.

2. Experimental details

2.1. Materials and analytical equipment

All the organic and organometallic reagents were pure commercial products. $[\{Rh(CO)_2Cl\}_2]$ was sublimed before use. The solvents were reagent grade and were dried and distilled by standard techniques before use. All manipulations of rhodium compounds and siloxanized reagents (prior to the sol–gel process) were carried out under dry dinitrogen by means of standard Schlenk-tube techniques.

Elemental analyses (C, H, N, S) were performed with a Carlo Erba EA 1108 automated analyzer. BET surface areas were measured using Micromeritics equipment. IR spectra were recorded on a Nicolet 5PC FT spectrometer; ^1H and ^{13}C NMR spectra were obtained with Bruker AC-100 and CXP-200 instruments; mass spectra were recorded on a Finnigan SSQ 710 mass spectrometer. Analytical GLC was carried out with a DANI 3900 chromatograph fitted with a methylsilicone (OV101) coated capillary column. Energy dispersive X-ray microanalyses (EDX) and scanning electron microscopy (SEM) images were obtained by the electron microscope microanalysis system JEOL 6400 EDS Tracor at the Institutes of Petrology, Mineralogy and Geology, University of Parma.

XPS spectra were run on a Vacuum Generators ESCALAB spectrometer, equipped with a hemispherical analyzer operated in the fixed analyzer transmission (FAT) mode, with a pass energy of 20 or 50 eV. Al $K\alpha_{1,2}$ or Mg $K\alpha_{1,2}$ photons ($h\nu$ = 1486.6 and 1253.6 eV, respectively) were used to excite photo-emission. The binding energy (*BE*) scale was calibrated by taking

the Au $4f_{7/2}$ peak at 84.0 eV. Correction of the energy shift due to static charging of the samples was accomplished by referencing to the C(1s) line from the residual pump line oil contamination, taken at 285.0 eV. The accuracy of reported *BE*s was ±0.2 eV, and the reproducibility of the results was within these values. The spectra were collected by a DEC PDP 11/83 data system and processed by means of VG 5000 data handling software.

2.2. Preparations and reactions

2.2.1. Preparation of $PhC(O)NHC(S)NH(CH_2)_2CH_3$ (Hbztu)

This ligand was prepared according to the method described in the literature [21b] with slight modifications. Propylamine (1.45 g, 24.5 mmol) was added dropwise to a toluene solution (20 ml) of benzoyl isothiocyanate (4 g, 24.5 mmol). An exothermal reaction took place and after 10 min a precipitate was formed. The mixture was allowed to react for 3 h and then filtered. The white precipitate was washed with isopropanol and dried in vacuo. Yield 60%. Analysis: Found (calc. for $C_{11}H_{14}N_2OS$): C, 60.9 (59.4); H, 6.4 (6.3); N, 12.4 (12.6); S, 14.1(14.4)%. MS *m/z* (CI, positive ions): 76 (100%) (M − 146); 223 (60%) (M + 1); 222 (16%) (M). FT-IR (KBr) (cm^{-1}) (thiourea group assignments following Jensen and Nielsen [22]): 3232 (br, s) (νNH); 3059 (w) (νCHarom); 2929 (mw), 2881 (w) (νCHaliph.); 1674 (s) (νCO); 1559 (s), 1535 (br, vs) (ν_{as}NCN, B band); 1258 (m) (ν_sNCN + νNH, C band); 1192 (ms) (ν_sNCS, D band); 696 (m) (ν_sCS + νNCN, F band). ^{1}H NMR ($CDCl_3$, TMS) δ: 10.80 (s, NH); 9.10 (s, NH); 7.93 (d, 1H, arom.); 7.86 (d, 1H, arom.); 7.67–7.48 (m, 3H, arom.); 3.72 (dt, NCH_2); 1.75 (sex, CH_2); 1.07 (t, CH_3) ppm. ^{13}C NMR ($CDCl_3$, TMS) δ: 179.7 (CS); 166.7 (CO); 133.4–127.3 (arom.); 47.5 (CH_2); 21.5 (CH_2); 11.4 (CH_3) ppm.

2.2.2. Preparation of [Rh(cod)(Hbztu)Cl] (1)

Hbztu (0.15 g) was allowed to react with $[\{Rh(cod)Cl\}_2]$ (0.17 g) in 5 ml of CH_2Cl_2 at room temperature for 1 h. Hexane was added to the orange solution obtained and after few hours orange crystals, suitable for X-ray analysis, were formed (80% yield). Analysis: Found: C, 50.3; H, 5.6; N, 5.9; S, 7.0%. $C_{19}ClH_{26}N_2ORhS$ requires: C, 48.7; H, 5.6; N, 6.0; S, 6.8%. FT-IR (KBr) (cm^{-1}): 3184 (br, m) (νNH); 3080 (w) (νCH arom.); 2932 (m), 2875 (w) (νCH aliph.); 2831 (νCH cod); 1669 (s) (νCO); 1573 (s), 1532 (br, vs) (B band); 1274 (m) (C band); 1194 (ms) (D band); 691 (m) (F band). ^{1}H NMR δ: 12.34 (s, NH); 11.30 (s, NH); 8.19 (d, 1H, arom.); 8.11 (d 1H, arom.); 7.67–7.42 (m, 3H, arom.); 4.41 (s, CH cod); 3.58 (dt, NCH_2); 2.53–1.57 (m, CH_2cod and CH_2CH_3); 1.02 (t, CH_3) ppm. ^{13}C NMR δ: 179.5 (CS); 170 (CO); 133.8–128.8 (arom.); 82.6 (CH cod); 47.4 ($NHCH_2$); 31.1 (CH_2 cod); 21.6 (CH_2CH_3); 11.6 (CH_3) ppm.

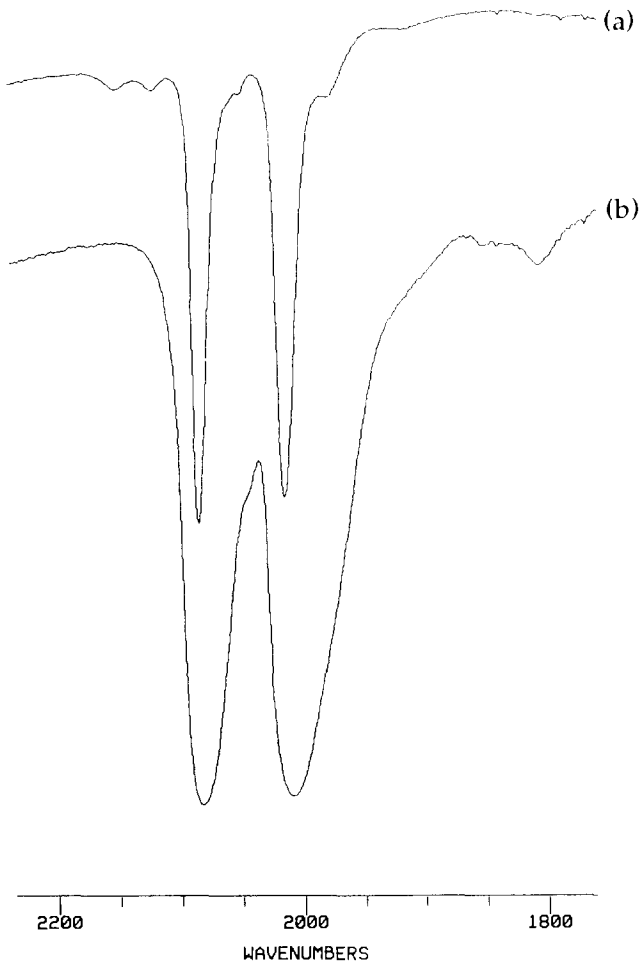

Fig. 1. Comparison between the IR spectra, in the carbonyl stretching region, of (a) the $Rh(CO)_2Cl$/Hbztu complex in dichloromethane solution (2087, 2018 cm^{-1}) and (b) the corresponding anchored species on XGbztu* (2083, 2010 cm^{-1}).

2.2.3. Reaction of Hbztu with $[\{Rh(CO)_2Cl\}_2]$

Hbztu (0.23 g) and 0.2 g of $[\{Rh(CO)_2Cl\}_2]$ (2:1 molar ratio) were dissolved under nitrogen atmosphere in 5 ml of CH_2Cl_2 and allowed to react at room temperature for 20 min. Addition of hexane gave an oily product. The formation of a 1:1 Hbztu–Rh complex similar to **1** is suggested by the IR spectrum (Fig. 1(a)) of the same solution: νCO (cm^{-1}): 2087 and 2018.

2.2.4. Reaction of Li[Bztu] with $[\{Rh(CO)_2Cl\}_2]$

Hbztu (0.10 g) was allowed to react with a solution consisting of 0.28 ml of LiBu (1.6 M in hexane) in 5 ml of distilled Et_2O at −70°C. A white precipitate was formed. It was dissolved in 2.5 ml of THF when a colourless solution was obtained. The medium–strong νCO band observed at 1670 cm^{-1} for the thiourea in THF disappeared owing to the formation of the

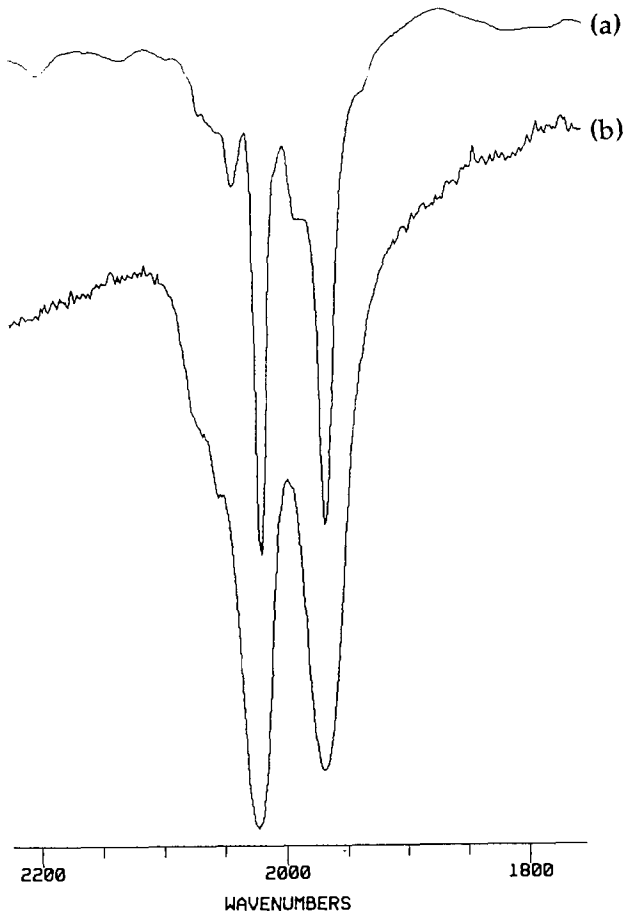

Fig. 2. Comparison between the IR spectra, in the carbonyl stretching region, of (a) the $Rh(CO)_2$/thioureato complex in tetrahydrofuran solution (2020, 1968 cm^{-1}) and (b) the Rh/XGbztu* catalyst after three cycles (2023, 1969 cm^{-1}).

thioureate anion. This solution was added to 0.087 g of $[\{Rh(CO)_2Cl\}_2]$ in 3 ml of THF and, after heating under reflux for 40 min, the FT-IR spectrum in THF (Fig. 2(a)) showed two strong and sharp bands at 2020 and 1968 cm^{-1}. An oily product was also obtained on addition of hexane.

2.2.5. Preparation of $[SiO_{3/2}(CH_2)_3NH_2]_n$

$(EtO)_3Si(CH_2)_3NH_2$ (90 mmol) was stirred with 10 ml of water and 10 ml of EtOH and warmed at 40–50°C. When a gel formed the warming was discontinued. Homogeneous gel formation occurred within 1 d; the gel (water-soluble) was then crushed, washed and dried in vacuo at 40°C for 20 min. Analysis: Found: C, 31.7; H, 7.5; N, 11.7%. $C_3H_8NO_{1.5}Si$ requires: C, 32.7; H, 9.1; N, 12.7%. FT-IR (KBr) (cm^{-1}): 3362 (br, w) (νNH); 2931 (m) (νCH); 1597 (ms) (δNH); 1029 (vs, br) (νSiO). MS *m/z* (CI, positive ions): 882 (100%, $n = 8$); 910 (16%); 984 (54%); 1103 (21%, $n = 10$).

2.2.6. Preparation of $[SiO_{3/2}(CH_2)_3NHC(S)NHC(O)Ph]_n$ (XGbztu)*

$[(SiO_{3/2}(CH_2)_3NH_2]_n$ (2.01 g) was added to a solution consisting of 2.45 ml of benzoyl isothiocyanate (12 mmol) in 30 ml of toluene. After heating under reflux for 6 h, the suspended solid was filtered and washed with toluene. Analytical and IR data revealed the presence of unreacted isothiocyanate and amine oligomers: Analysis: Found: C, 45.9; H, 5.1; N, 10.4; S, 8.3%. FT-IR (KBr) (cm^{-1}); 3244 (br, w) (νNH); 2930 (mw) (νCHalif.); 2060 (m) (νNCS); 1672 (s) (νCO); 1555, 1520 (s) (band B); 1024 (vs, br) (νSiO); 692 (m) (band F). To remove these impurities, the xerogel was treated with EtOH in a Soxhlet apparatus for 5 d and then dried in vacuo. Analysis: Found: C, 50.5; H, 4.8; N, 9.6; S, 10.2%. $C_{11}H_{13}N_2O_{2.5}SSi$ requires: C, 48.4; H, 4.8; N, 10.3; S, 11.7%. FT-IR (cm^{-1}); 3247 (br, w) (νNH); 2927 (m) (νCH alif.); 1672 (s) (νCO); 1555, 1520 (s) (band B); 1024 (vs, br) (νSiO); 691 (m) (band F). MS *m/z* (EtOH solution after extraction): 882 (100%); 1103 (65%), corresponding, respectively, to the octamer and the decamer of $[(SiO_{3/2}(CH_2)_3NH_2]_n$.

2.2.7. Preparation of XGbztu (thiourea function diluted)

$(EtO)_3Si(CH_2)_3NH_2$ (2.1 g, 9.3 mmol) and 2.4 g (14.9 mmol) of benzoyl isothiocyanate were mixed together under dry dinitrogen. An exothermal reaction occurred and a yellow oil (crude $(EtO)_3Si(CH_2)_3NHC(S)NHC(O)Ph$) was obtained; then 7.7 g (36.9 mmol) of tetraethoxysilane were added. The mixture was stirred for a few minutes and then added to a solution consisting of 0.17 g of NH_4F in 7.50 ml of water. EtOH was added until a single phase was formed, which gelled in a few hours. The xerogel obtained was crushed, washed with water and dried in vacuo at 80°C. This glassy material was further purified by extraction with toluene for 2 d in a Sohxlet apparatus. Analysis: Found % (calc. for $4.5SiO_2 \cdot SiO_{1.5}C_{11}H_{13}N_2OS$): C, 24.5 (24.3); H, 2.7 (2.4); N, 4.5 (5.2); S, 4.9 (5.9%). FT-IR (KBr) (cm^{-1}): 3425 (s, vbr) (νOH); 3271 (sh) (νNH); 1676 (ms) (νCO); 1559 (s, br), 1524 (s) (ν_{as}NCN, B band); 1082 (vs, vbr) (νSiO); 715 and/or 665 (w) (ν_sCS + νNCN, F band). Surface area (BET): 70 $m^2\ g^{-1}$.

2.2.8. Anchoring rhodium from $[\{Rh(cod)Cl\}]_2$. Preparation of Rh / XGbztu and Rh / XGbztu*

The procedure was the same for XGbztu* and XGbztu. A stoichiometric amount of xerogel (Rh/S, 1:1 molar ratio) was suspended by magnetic stirring in a dichloromethane (or 1,2-dichloroethane) solution of $[\{Rh(cod)Cl\}_2]$. The mixture was allowed to react by heating under reflux for a few hours. The resulting orange solid (Rh/XGbztu* or Rh/XGbztu) was then filtered, washed with dichloromethane and dried in vacuo. Characterization of Rh/XGbztu*: atomic ratios

found by EDX microanalysis: Si/S, 1.3; Rh/Cl, 0.9; Rh/S, 0.5, FT-IR (KBr) (cm^{-1}): 3224 (br, w) (νNH); 2930, 2874 (m) (νCH); 1670 (s) (νCO); 1568 (s), 1531 (s) (band B); 1024 (vs, br) (νSiO); 710 (m) (band F). Characterization of Rh/XGbztu: atomic ratios found by EDX microanalysis: Si/S, 5.2; Rh/Cl, 0.9; Rh/S, 0.4. FT-IR (cm^{-1}); 3405 (br, w) (νNH and νOH); 2940 (w) (νCHalif.); 1680 (m) (νCO); 1576 (m), 1540 (m) (band B); 1088 (vs, vbr) (νSiO). XPS data are reported in Table 1.

2.2.9. Anchoring rhodium from $[\{Rh(CO)_2Cl\}]_2$ to XGbztu*

The xerogel was suspended by magnetic stirring in a THF solution containing a stoichiometric amount of $[\{Rh(CO)Cl\}_2]$ (Rh/S, 1:1 molar ratio). The mixture was allowed to react at room temperature for a few hours and then filtered. The solid orange product was washed with dichloromethane and dried in vacuo. The FT-IR spectrum in KBr showed two strong bands due to ν(CO) at 2083 and 2010 cm^{-1}, which suggest the presence on the xerogel surface of an anchored rhodium species similar to the complex obtained with Hbztu. A comparison of the spectra of these two systems is shown in Fig. 1.

2.2.10. Hydroformylation reactions

The hydroformylation reactions were performed in a 50 ml stainless-steel autoclave (Parr) equipped with a magnetic stirrer and thermostated (±1°C) in a silicone oil bath (Fischer). Yield and selectivity were determined by GLC using internal standards.

In a typical run, distilled styrene (2 g), toluene (3 ml) and the xerogel (0.08 g of Rh/XGbztu or 0.04 g of Rh/XGbztu*) were introduced under dinitrogen in the autoclave to achieve an approximate styrene/Rh ratio of 300:1. After some pressurization and evacuation, the autoclave was charged at −20°C with dihydrogen and carbon monoxide (1:1) at 60 atm (pressure at room temperature). The reaction mixture was stirred at 80°C for 10–12 h, then filtered and analyzed by GLC. The recovered solid catalyst was re-used in a further run. For all the catalytic runs, the styrene conversion was about 99% and the yield in the two isomeric aldehydes was about 98%. Trace amounts of ethylbenzene (< 1%) were detected. The iso/normal selectivity data are reported in Fig. 3. The recovered catalysts were analyzed by IR spectroscopy: Fig. 4 shows the IR patterns of the Ru/XGbztu* system after three consecutive catalytic cycles. XPS data for Rh/XGbztu are quoted in Table 1 and Fig. 5 shows the Rh(3d) pattern. Finally, Fig. 6 shows an SEM image and the EDX spectrum of Rh/XGbztu* after three cycles.

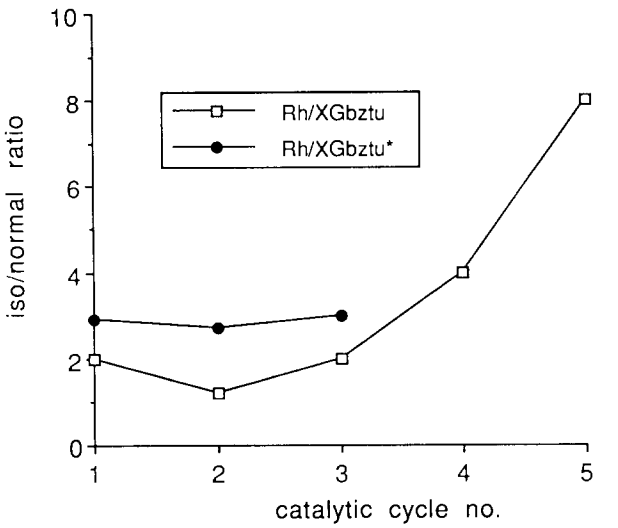

Fig. 3. Iso/normal selectivity ratio versus catalytic cycle number in the hydroformylation of styrene catalyzed by Rh/XGbztu and XGbztu*.

2.3. X-ray data collection, structure determination and refinement for [Rh(cod)(Hbztu)Cl] (1)

Suitable deep orange crystals for X-ray analysis were obtained directly from the preparation mixture. The crystallographic data are summarized in Table 2. Data were collected at room temperature (22°C) on a Philips PW1100 diffractometer, using graphite monochromated Mo Kα radiation and the $\theta/2\theta$ scan type. The reflections were collected with a variable scan speed of 3–12° min^{-1} and a scan width from $(\theta - 0.65)°$ to $(\theta + 0.65 + 0.346 \tan \theta)°$. One standard reflection was monitored every 100 measurements; no significant decay was noticed over the time of data collection. The

Table 1
XPS data [*BE* (eV) and atomic ratios [a]] for XGbztu and its rhodium derivatives

Compound	N(1s)	S(2p)	$Rh(3d_{5/2})$	N/S	Si/N	Rh/S	Rh/Si	Rh^+/Rh^{3+}
XGbztu	400.3	162.5	–	3.7	2.8	–	–	–
Rh/XGbztu	400.2	163.1	309.1	3.4	2.8	1.2	0.1	–
Rh/XGbztu/5 [b]	400.9	169.9	308.7 (Rh^+) 310.3 (Rh^{+3})	3.6	3.2	1.0	0.1	2.4

[a] Experimental errors on binding energies, ±0.2 eV; on atomic ratios, ±10%–20%.
[b] Catalyst recovered after the fifth hydroformylation cycle.

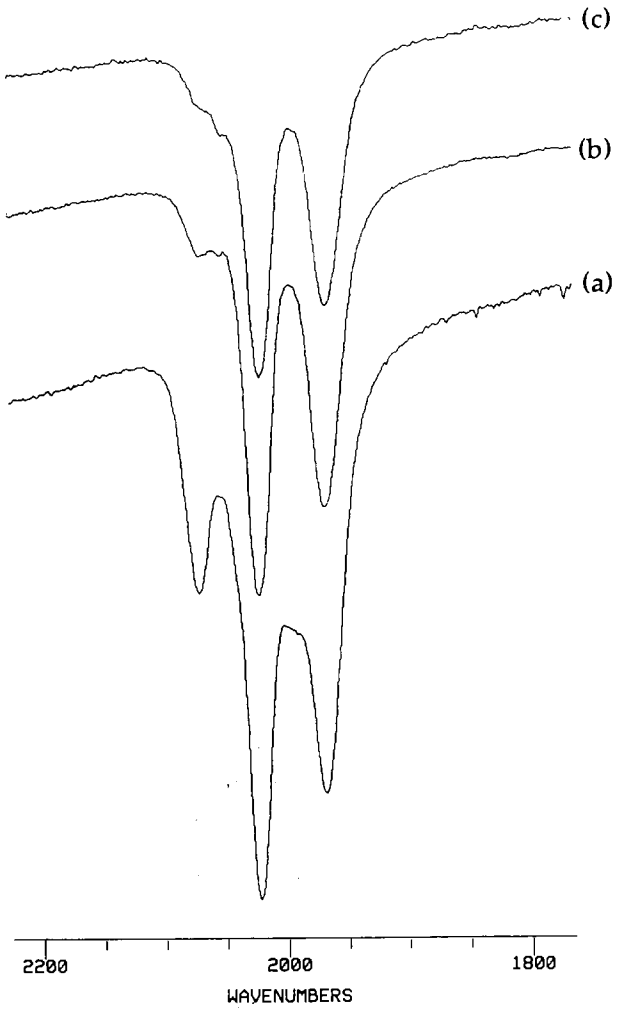

Fig. 4. IR patterns of the Rh/XGbztu* system after three consecutive catalytic cycles (a–c), emphasizing the progressive transformation of the thiourea–carbonyl rhodium complex (derived from the corresponding starting cod complex; only the peak at 2076 cm^{-1} is detectable) into the hypothetical, lower ν(CO) frequency thioureato species (2023, 1969 cm^{-1}).

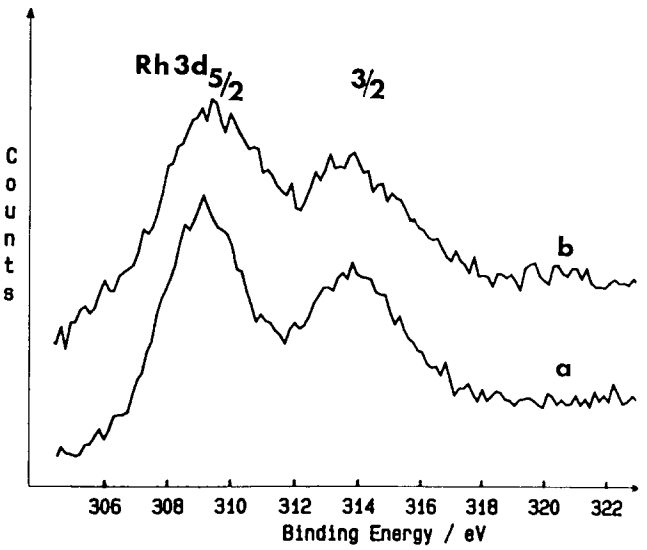

Fig. 5. Rh(3d) XPS patterns of the fresh Rh/XGbztu system (a) and after five catalytic cycles (b). Note the asymmetry of the peaks in (b), which is due to a higher *BE* component (see Table 1).

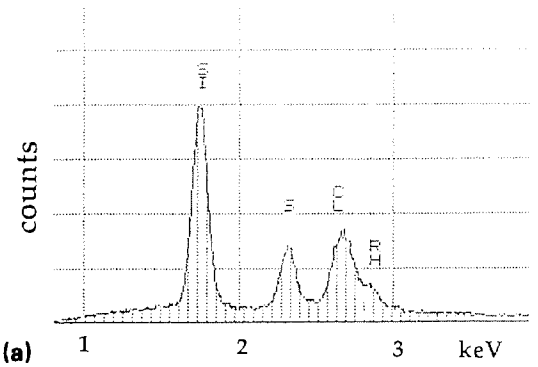

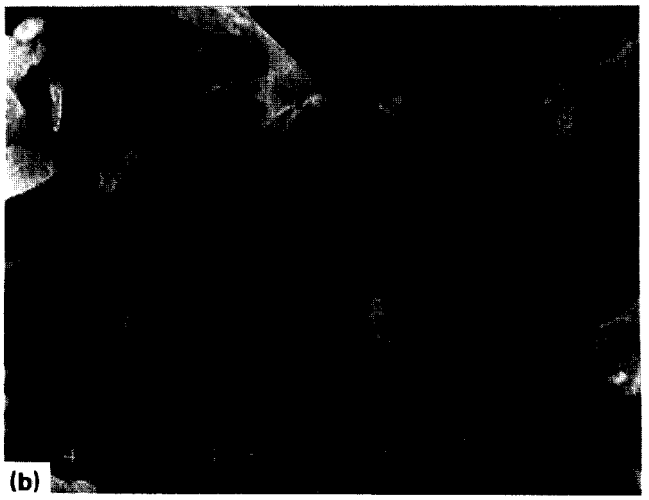

Fig. 6. (a) EDX spectrum and (b) SEM view of the Rh/XGbztu* system after three catalytic cycles; atomic ratios: Si/S, 2.5;Rh/Cl, 0.8; Rh/S, 0.7; Si/Rh, 3.4.

individual profiles have been analyzed following Lehmann and Larsen [23]. Intensities were corrected for Lorentz and polarization effects; no correction for absorption was necessary. Only the observed reflections were used in the structure solution and refinement.

The structure was solved by Patterson and Fourier methods and refined by full-matrix least-squares first with isotropic thermal parameters and then with anisotropic thermal parameters for all non-hydrogen atoms. All hydrogen atoms were clearly localized in the final ΔF map and refined isotropically. In the final cycles of refinement a weighting scheme, $w = [\sigma^2(F_o) + gF_o^2]^{-1}$ was used; at convergence the g value was 0.0070. The analytical scattering factors, corrected for the real and imaginary parts of anomalous dispersions, were taken from Ref. [24]. All calculations were car-

ried out on the GOULD POWERNODE 6040 of the "Centro di Studio per la Strutturistica Diffrattometrica" del CNR, Parma, using the SHELX-76 and SHELXS-86 systems of crystallographic computer programs [25]. The final atomic coordinates for the non-hydrogen atoms are listed in Table 3. Additional data (atomic coordinates of the hydrogen atoms, thermal parameters) have been deposited at the Cambridge Crystallographic Data Centre or are available from the authors.

3. Results and discussion

3.1. Functionalized materials and rhodium complexes

The benzoylthiourea Hbztu has been prepared as a suitable molecular model for the tethered functions of the silica xerogels XGbztu and XGbtzu*. Because of the synthetic conditions adopted both xerogels must be carefully cleaned in order to remove some unreacted isothiocyanate and, in the case of XGbztu*, some unreacted $[SiO_{3/2}(CH_2)_3NH_2]_n$. This material, which is soluble in water and light alcohols, consists of a mixture of oligomeric molecules, the pseudo-cubic octamer being the main component [26]. This is suggested by the chemical ionization positive ion mass spectrum of the mixture, which shows the highest peak due to the octamer at m/z 882 (M + 2). The corresponding benzoylthiourea-functionalized material is quite insoluble in common solvents but, owing to its oligomeric nature, its surface area is almost zero. In contrast, the xerogel XGbztu, obtained by hydrolysis and co-condensation of the crude triethoxysilylpropylbenzoylthiourea with tetraethoxysilane, exhibits a surface area of 70 $m^2\ g^{-1}$. The integrity of the tethered benzoylthiourea group in the two purified materials is confirmed by the presence in their IR spectra of bands typical of this function, which appear at nearly the same frequency as in the model compound Hbztu. In particular, the ν(CO) and the thiourea B bands are easily identified in the IR spectra of the xerogels, whereas the other thiourea bands are masked by the strong and broad absorption of the Si—O groups centered at ca. 1080 cm^{-1}.

Hbztu reacts with $[\{Rh(cod)Cl\}_2]$ giving the 1:1 thiourea/rhodium complex **1** characterized by elemental analysis and IR and NMR spectroscopy. In particular, the high frequency shift of the B and C bands in **1** with respect to the free thiourea suggests sulfur coordination, the carbonyl group being engaged in an intramolecular hydrogen bond as confirmed by its crystal structure (vide infra). Similarly, Hbztu reacts with 1 equiv. of $[\{Rh(CO)_2Cl\}_2]$ giving a product which shows two strong carbonyl stretching bands at 2087 and 2018 cm^{-1} in solution as required by a complex of the type $[Rh(CO)_2(L)Cl]$ [27]. An oily material was obtained on evaporation of the solvent under vacuum, as in the case

Table 2
Summary of crystallographic data for complex **1**

Formula	$C_{19}H_{26}ClN_2ORhS$
Mol. wt.	468.85
Crystal system	triclinic
Space group	$P\bar{1}$
Radiation (λ Å)	graphite monochromated Mo Kα (0.71073)
a, Å	7.005(2)
b, Å	9.341(2)
c, Å	16.198(4)
α, deg	73.36(2)
β, deg	78.55(2)
γ, deg	85.39(2)
V, Å^3	995.0(5)
Z	2
D_{calc}, g cm^{-3}	1.565
F(000)	480
Cryst. size, mm	0.14 × 0.22 × 0.23
μ(Mo Kα), cm^{-1}	11.07
Diffractometer	Philips
2θ range, deg	6–60
Reflections measured	$\pm h, \pm k, l$
Unique total data	5820
Unique observed data [$I > 2\sigma(I)$]	3844
R	0.0380
R_W	0.0486

Table 3
Fractional atomic coordinates (×10^4) and equivalent thermal parameters (Å^2 × 10^4) for the complex [Rh(Hbztu) (cod)Cl]

Atom	x	y	z	U_{eq}
Rh	907.5(4)	2952.7(3)	1600.9(2)	334(1)
Cl	−2093.2(14)	2654.8(14)	2620.1(7)	556(4)
S	2014.7(16)	4946.2(11)	2015.2(6)	479(3)
O	1739(5)	3606(4)	4960(2)	653(13)
N(1)	3040(6)	5398(4)	3396(2)	535(13)
N(2)	649(4)	3652(4)	3714(2)	387(10)
C(1)	1919(5)	4661(4)	3108(2)	377(12)
C(2)	4440(8)	6526(6)	2859(3)	641(19)
C(3)	6294(7)	6326(5)	3205(3)	562(17)
C(4)	7700(8)	7578(6)	2685(4)	650(21)
C(5)	588(5)	3184(4)	4615(2)	423(12)
C(6)	−960(5)	2110(4)	5126(2)	381(11)
C(7)	−2794(6)	2209(5)	4916(2)	445(13)
C(8)	−4211(7)	1200(5)	5441(3)	537(16)
C(9)	−3760(7)	96(5)	6152(3)	567(17)
C(10)	−1928(7)	7(5)	6359(3)	548(16)
C(11)	−529(6)	1013(5)	5860(3)	478(14)
C(12)	500(7)	897(5)	1324(3)	530(16)
C(13)	−360(7)	2056(5)	764(3)	525(17)
C(14)	558(11)	2774(9)	−189(3)	837(27)
C(15)	2544(10)	3286(8)	−342(3)	812(25)
C(16)	3095(7)	3567(6)	462(3)	544(16)
C(17)	3831(6)	2469(6)	1106(3)	569(18)
C(18)	4145(9)	848(7)	1141(5)	796(27)
C(19)	2406(10)	124(7)	1028(5)	767(25)

of diphenylthiourea [19], and no other attempts were made to isolate a solid product.

On the other hand, both xerogels XGbztu and XGbztu* react with $[\{Rh(cod)Cl\}_2]$ producing the hybrid materials Rh/XGbztu and Rh/XGbztu*, respectively. They contain anchored metal complexes of the same nature as **1**, as suggested by their IR spectra. Sulfur coordination is also indicated by the significant increase in the S(2p) binding energy in the XPS spectrum of Rh/XGbztu relative to the unreacted xerogel (Table 1). In Rh/XGbztu, the Rh/S atomic ratio observed by EDX (0.4) is significantly lower than that found by XPS (1.2). This apparent discrepancy is due to the different surface depths explored by the two techniques (~ 5 nm for XPS and ~ 1000 nm for EDX), and indicates clearly that a considerable fraction of the thiourea groups in the inner layers of the gel is not accessed by the rhodium species. Also $[\{Rh(CO)_2Cl\}_2]$ reacts with XGbztu* to afford an anchored carbonyl complex whose two IR ν(CO) bands (2083 and 2010 cm^{-1}) are near the frequencies found for the rhodium carbonyl complex of Hbztu (2087 and 2018 cm^{-1}) as shown in Fig. 1.

3.2. Description of the crystal structure of [Rh(cod)(Hbztu)Cl] (1)

As mentioned above, complex **1** represents a suitable molecular model of the anchored species of the composite materials Rh/XGbztu and Rh/XGbztu*, so its X-ray structure was determined and is shown in Fig. 7 together with the atomic labelling scheme. Selected bond distances and angles are listed in Table 4. The Rh atom is coordinated by a Cl atom, an S atom from the Hbztu molecule and by the cod interacting through the two double bonds. If the midpoints of these double bonds, M(1) and M(2), are taken into account, the Rh atoms display a slightly distorted square-planar coordination. An intramolecular hydrogen bond is formed by the N(2) atom with the Cl atom [N(2)—H $\cdots$ Cl = 3.207(4) Å, N(2)—H—Cl = 163(4)°]. The value of the Rh—S bond, 2.382(1) Å, is comparable with those found in the structure of the complex $[\{RhCl(CO)_2\}_2\{\mu\text{-}SC(NHPh)(NH^nPr)\}]$, 2.386(2) and 2.420(2) Å [19], in which the sulfur of the phenylpropylthiourea bridges two $RhCl(CO)_2$ units. In the thiourea moiety, the value of C—S bond distance, 1.701(4) Å, is slightly longer than in the free Hbztu, 1.678(4) Å [21a], consistent with decreasing double-bond character with respect to free thiourea, whereas the values of the C—N bond lengths, 1.314(6) and 1.380(4) Å, slightly shorter than in free Hbztu, 1.332(7) and 1.393(5) Å, indicate a slight increase of the multiple-bond character with respect to free thiourea. The difference in the two C—N bond lengths, as already observed in other complexes [28] and in free Hbztu, indicates a greater C—N double-bond character in the bond not adjacent to the carbonyl group, whereas in the substituted thioureas the orders of these two bonds are very close. As in the free molecule, the conformation of Hbztu in **1** is essentially determined by the formation of an intramolecular N(1)—H $\cdots$ O hydrogen bond [N(1)—H $\cdots$ O = 2.636(4) Å, N(1)—H—O = 135(5)°]. The thiourea moiety is tilted by 9.8(1)° with respect to the amide group and this latter is tilted by 35.9(2)° with respect to the phenyl group.

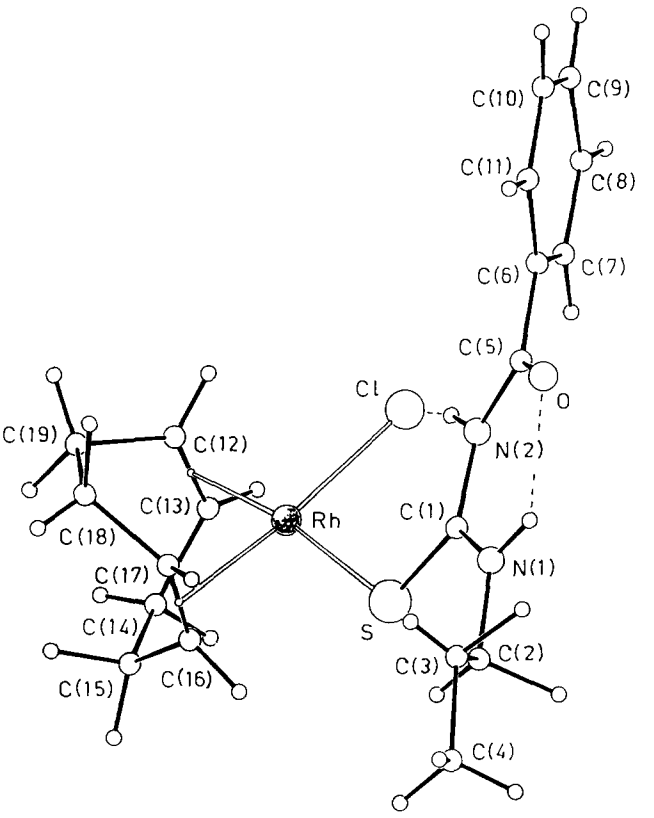

Fig. 7. View of the molecular structure of [Rh(cod)(Hbztu)Cl] (1) together with the atomic numbering scheme.

3.3. Hydroformylation reactions

The rhodium-containing composite materials Rh/XGbztu and Rh/XGbztu* are effective hydroformylation catalyst precursors, styrene being quantitatively converted into the corresponding linear (normal) and branched (iso) aldehydes under relatively mild conditions. Although the catalysts can be easily recovered by filtration and re-used without loss of activity, major changes occur to the tethered rhodium species mainly in the system Rh/XGbztu, as shown by spectroscopic data. This is accompanied by significant changes in the iso/normal selectivity ratio for this catalyst (Fig. 3).

Table 4
Selected bond distances (Å) and angles (°) for the complex [Rh(Hbztu) (cod) Cl]

Rh—Cl	2.382(1)	Rh—S	2.382(1)
Rh—M(1) [a]	2.028(6)	Rh—M(2) [a]	1.997(4)
Rh—C(12)	2.146(5)	Rh—C(16)	2.119(4)
Rh—C(13)	2.139(6)	Rh—C(17)	2.109(4)
S—C(1)	1.701(4)	C(8)—C(9)	1.378(6)
O—C(5)	1.214(6)	C(9)—C(10)	1.380(8)
N(1)—C(1)	1.314(6)	C(10)—C(11)	1.377(6)
N(1)—C(2)	1.460(6)	C(12)—C(13)	1.381(6)
N(2)—C(1)	1.380(4)	C(12)—C(19)	1.524(8)
N(2)—C(5)	1.390(5)	C(13)—C(14)	1.525(6)
C(2)—C(3)	1.491(8)	C(14)—C(15)	1.459(11)
C(3)—C(4)	1.530(7)	C(15)—C(16)	1.525(8)
C(5)—C(6)	1.486(5)	C(16)—C(17)	1.386(6)
C(6)—C(7)	1.383(6)	C(17)—C(18)	1.499(9)
C(6)—C(11)	1.395(5)	C(18)—C(19)	1.505(11)
C(7)—C(8)	1.397(6)		
M(1)—Rh—M(2) [a]	87.2(2)	C(5)—C(6)—C(7)	122.2(4)
S—Rh—M(2)	87.2(2)	C(7)—C(6)—C(11)	120.2(4)
S—Rh—Cl	95.78(4)	C(6)—C(7)—C(8)	119.6(4)
Cl—Rh—M(1)	90.3(1)	C(7)—C(8)—C(9)	119.9(4)
Rh—S—C(1)	115.9(1)	C(8)—C(9)—C(10)	120.2(5)
C(1)—N(1)—C(2)	126.3(4)	C(9)—C(10)—C(11)	120.6(5)
C(1)—N(2)—C(5)	126.3(3)	C(6)—C(11)—C(10)	119.5(4)
N(1)—C(1)—N(2)	118.3(4)	C(13)—C(12)—C(19)	122.9(5)
S—C(1)—N(2)	120.6(3)	C(12)—C(13)—C(14)	124.0(4)
S—C(1)—N(1)	121.1(3)	C(13)—C(14)—C(15)	116.1(5)
N(1)—C(2)—C(3)	111.1(5)	C(14)—C(15)—C(16)	113.4(5)
C(2)—C(3)—C(4)	111.1(5)	C(15)—C(16)—C(17)	123.8(4)
O—C(5)—N(2)	122.3(3)	C(16)—C(17)—C(18)	126.2(5)
N(2)—C(5)—C(6)	115.6(3)	C(17)—C(18)—C(19)	114.3(6)
O—C(5)—C(6)	122.1(4)	C(12)—C(19)—C(18)	111.9(5)
C(5)—C(6)—C(11)	117.6(3)		

[a] M(1) and M(2) are the midpoints of the bonds C(12)=C(13) and C(16)=C(17), respectively.

In both materials, after the first catalytic cycle, the starting anchored cod complexes have already been turned into carbonyl species. Simple substitution of cod by CO should give the corresponding carbonyl chloro complex characterized by the two ν(CO) bands at 2083 and 2010 cm^{-1} and shown in Fig. 1(b) for XGbztu*. These are [Fig. 4(a)] accompanied by two more intense low-frequency bands (2028, 1974 for XGbztu and 2023, 1969 cm^{-1} for XGbztu*), which recall the IR pattern obtained in solution by reaction of Li[bztu] with 1 equiv. of $[\{Rh(CO)_2Cl\}_2]$ (Fig. 2(a)). This suggests that thioureato complexes of the type depicted in the Scheme 2 should be present on the xerogel surface. At this stage (first cycle) the iso/normal selectivity is 3:1 for XGbztu* and 2:1 for XGbztu.

During further catalytic cycles other significant, but different changes occur in the IR spectrum of both xerogels. As shown in Fig. 4, in the case of Rh/XGbztu* complete conversion of the rhodium complexes into the thioureato species takes place at the second catalytic cycle, the selectivity remaining almost the same.

However, in the case of Rh/XGbztu, the two low-frequency bands attributed to the thioureato complex decrease in strength and a new broad band appears at 2080 cm^{-1} and grows stronger. At the same time, for the Rh/XGbztu system the iso/normal selectivity ratio increases, reaching 8:1 at the fifth cycle. The high-frequency broad band can be attributed both to tethered isothiocyanate groups and to silica-anchored carbonyl rhodium (III) species, possibly produced by oxidative attack of the surface silanol groups on the thioureato complexes. This last hypothesis is also substantiated by the XPS spectrum recorded for Rh/XGbztu after the fifth cycle (Table 1 and Fig. 5), in which the Rh(3d) peaks are broader than in the starting material, owing to the presence of a higher *BE* component attributable to rhodium(III) species [29]. The data quoted in Table 1 show that after five cycles the organic function of XGbztu has also undergone considerable deterioration, thiourea sulfur being completely converted to an oxidized species with a *BE* value of 169.9 eV.

In the case of the oligomeric material Rh/XGbztu*, the thioureato complexes appear to be more stable, no degradation to oxidized rhodium species being detectable by XPS after three cycles, probably because of the absence of a silanol group in this *superfunctionalized* xerogel. Nevertheless, some metal and sulfur leaching occurs, as indicated by the EDX atomic ratios Si/S and Si/Rh for the starting material (1.4 and 2.5) and after three catalytic runs (2.5 and 3.4, Fig. 6). For the surface layers explored by XPS, metal and sulfur leaching appears more pronounced, the Si/Rh and Si/S(total) atomic ratios being 4.2 and 7.6, respectively (Rh/S(total), 1.8; N/S(total), 5.2; Si/N, 1.5). As stated above, only rhodium(I) is present (309.1 eV), whereas the S(2p) peak appears double [S(tu), 163.6; S(ox) 168.4 eV; S(tu)/S(ox), 1.05] as a result of the formation of an oxidized sulfur species. The SEM view of the material after three catalytic cycles is shown in Fig. 6 along with the EDX pattern: glassy grains of micrometre size are

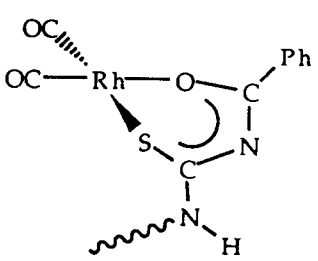

Scheme 2.

evident. Moreover, despite to the hypothetical formation of the anchored thioureato species, chlorine is still present, probably as hydrochloric acid neutralized by the basic functions (e.g., free thioureas) of the xerogel.

4. Conclusions

In conclusion, new benzoylthiourea-functionalized hybrid materials have been prepared by the sol–gel process. The anchoring of rhodium affords recyclable sulfur-ligand hydroformylation catalysts (only tested for styrene) which exhibit remarkably different behaviours depending on the density of the benzoylthiourea function on these xerogels. Fast degradation of the ligand functionality occurs in the diluted system XGbztu, whereas the *superfunctionalized* material XGbztu* appears more stable towards these undesired processes, even if some metal and sulfur leaching occurs. These preliminary results suggest that the formation of rhodium(III) species on the silica surface of XGbztu could promote the decomposition of the benzoylthiourea function, whose S(2p) and N(1s) peaks completely disappear after five cycles. In the case of XGbztu*, the main degradation process should only be due to the intrinsic fragility of the benzoylthiourea function, whose decomposition, as shown by loss of sulfur, is apparently responsible for some rhodium leaching.

Further investigations are in progress in order to exploit the potential of such sulfur-ligand metal catalysts under different experimental conditions with different organic substrates and with simpler and more stable thiourea functions. Moreover, comparative experiments with the corresponding homogeneous catalysts should give more information about the nature of the active species.

Acknowledgments

Financial support from CNR (Rome), Progetto Finalizzato Chimica Fine II, and from MURST (Rome) is acknowledged. The facilities of Centro Interdipartimentale Misure (University of Parma) were used for recording NMR and mass spectra.

References

[1] Yu.I. Yermakov, B.N. Kuznetsov and V.A. Zakharov, *Catalysis by Supported Complexes*, Elsevier, Amsterdam, 1981.
[2] F.R. Hartley, *Supported Metal Complexes*, Reidel, Dordrecht, 1985.
[3] D.C. Bailey and S.H. Langer, *Chem Rev.*, 81 (1981) 109.
[4] R.H. Grubbs, *Chemtech*, (1977) 512.
[5] C.U. Pittman, in G. Wilkinson, F.G.A. Stone and E.W. Abel (eds.), *Comprehensive Organometallic Chemistry*, Pergamon, Oxford, 1982, Vol. 8, Chap. 55.
[6] M. Capka, P. Svoboda, M. Kraus and J. Hetflejs, *Chem. Ind. (London)*, (1972) 650; N.L. Holy, *Chemtech* (1980) 366.
[7] M. Capka and J. Hetflejs, *Collect. Czech. Chem. Commun., 39* (1974) 154.
[8] B. Corain, M. Basato, M. Zecca, G. Braca, M. Raspolli Galletti, S. Lora, G. Palma and G. Guglielminotti, *J. Mol. Catal., 73* (1993) 23.
[9] L.L. Hench and J.K. West, *Chem. Rev., 90* (1990) 33.
[10] R.J.P. Corriu, J.J.E. Moreau, P. Thepot and M.W. Chi Man, *Chem. Mater., 4* (1992) 1217; K.J. Shea, D.A. Loy and O. Webster, *J. Am. Chem. Soc., 114* (1992) 6700.
[11] I.S. Khatib and R.V. Parish, *J. Organomet. Chem., 369* (1989) 9.
[12] (a) U. Schubert, K. Rose and H. Schmidt, *J. Non-Cryst. Solids, 105* (1988) 165; (b) U. Schubert, C. Egger and K. Rose, C. Alt, *J. Mol. Catal., 55* (1989) 330; (c) R.V. Parish, D. Habibi and V. Mohammadi, *J. Organomet. Chem., 369* (1989) 17; (d) H.S. Hilal, A. Rabah, I.S. Khatib and A.F. Schreiner, *J. Mol. Catal., 61* (1990) 1; (e) J.R. Hardee, S.E. Tunney, J. Frye and J.K. Stille, *J. Polym. Sci., Polym. Chem. Ed., 28* (1990) 3669; (f) M. Capka, M. Czakoova, W. Urbaniak and U. Schubert, *J. Mol. Catal., 74* (1992) 335.
[13] (a) H. Tamagawa, K. Oyama, T. Yamaguchi, H. Tanaka, H. Tsuiki and A. Ueno, *J. Chem. Soc., Faraday Trans. 1, 83* (1987) 3189; (b) U. Schubert, S. Amberg-Schwab and B. Breitscheidel, *Chem. Mater., 1* (1989) 576; (c) T. Lopez, P. Bosch and R. Gomez, *React. Kinet. Catal. Lett., 41* (1990) 217; (d) T. Lopez, A. Lopez-Gaona and R. Gomez, *Langmuir, 6* (1990) 1343; (e) J.M. Tour, S.L. Pendalwar and J.P. Cooper, *Chem. Mater., 55* (1990) 3452; (f) B. Breitscheidel, J. Zieder and U. Schubert, *Chem. Mater., 3* (1991) 559.
[14] T. Castrillo, H. Knözinger, M. Wolf and B. Tesche, *J. Mol. Catal., 11* (1981) 151; J. Evans and B.P. Gracey, *J. Chem. Soc., Chem. Commun.*, (1983) 247; U. Kiiski, T.A. Pakkanen and O. Krause, *J. Mol. Catal., 50* (1989) 143; E. Lindner, A. Bader and H. Mayer, *Inorg. Chem., 30* (1991) 3783.
[15] P. Hernan, C. del Pino and E. Ruiz-Hitzky, *Chem. Mater., 4* (1992) 49.
[16] T. Catrillo, K. Knözinger and M. Wolf, *Inorg. Chim. Acta, 45* (1980) L235; J. Evans and B.P. Gracey, *J. Chem. Soc., Dalton Trans.*, (1982) 1123; H.J. Zong, X.Y. Guo, Q. Tang, Y. Jin, Y.J. Li and Y.Y. Jiang, *J. Macromol. Sci. Chem., A24*, (1987) 277.
[17] C. Ferrari, G. Predieri, A. Tiripicchio and M. Costa, *Chem. Mater., 4* (1992) 243.
[18] M. Biagini Cingi, G. Peoni, G. Predieri, A. Tiripicchio and M. Tiripicchio Camellini, *Gazz. Chim. Ital., 122* (1992) 521; D. Cauzzi, G. Predieri, A. Tiripicchio, R. Zanoni and C. Giori, *Inorg. Chim. Acta, 221* (1994) 183.
[19] D. Cauzzi, M.A. Pellinghelli, G. Predieri and A. Tiripicchio, *Gazz. Chim. Ital., 123* (1993) 713.
[20] E. Boroni, G. Predieri, A. Tiripicchio and M. Tiripicchio Camellini, *Organometallics, 11* (1992) 3456; E. Boroni, G. Predieri, A. Tiripicchio and M. Tiripicchio Camellini, *J. Organomet. Chem., 451* (1993) 163.
[21] (a) A. Dago, Yu. Shepelev, F. Fajardo, F. Alvarez, R. Pomes, *Acta Crystallogr., C45*, (1989) 1192; (b) A. Macias, E. Otazo and I.P. Beletskaya, *Zh. Org. Khim., 18* (1982) 905.
[22] K.A. Jensen and P.H. Nielsen, *Acta Chem. Scand., 20* (1966) 597.
[23] M.S. Lehmann and F.K. Larsen, *Acta Crystallogr., Sect. A, 30* (1974) 580.
[24] *International Tables for X-Ray Crystallography*, Vol IV, Kynoch, Birmingham, 1974.
[25] G.M. Sheldrick, SHELX-76 *Program for Crystal Structure Determination*, University of Cambridge, England, 1976; SHELXS-86

Program for the Solution of Crystal Structures, University of Göttingen, 1986.

[26] H. Behbehani, B.J. Brisdon, M.F. Mahon and K.C. Molloy, *J. Organomet. Chem.*, *469* (1994) 19, and references therein.

[27] R.P. Hughes, in G. Wilkinson, F.G.A. Stone and E.W. Abel (eds.), *Comprehensive Organometallic Chemistry*, Pergamon, Oxford, 1983, Vol. 5, pp. 285 and 290.

[28] D. Cauzzi, M. Lanfranchi, G. Marzolini, G. Predieri, A. Tiripicchio, M. Tiripicchio Camellini, *Gazz. Chim. Ital.*, in the press.

[29] M. Kawai, M. Uda and M. Ichikawa, *J. Phys. Chem.*, *89* (1985) 1654.